Proceedings of the 17th International Symposium on the Packaging and Transportation of Radioactive Materials
PATRAM 2013
August 18-23, 2013, San Francisco, CA, USA

DEVELOPMENT OF A FINITE ELEMENT MODEL FOR DAMPING CONCRETE UNDER SEVERE IMPACT LOADS

Linan Qiao **Uwe Zencker**

Eva-Maria Kasparek **Holger Völzke** **Robert Scheidemann**

BAM Federal Institute for Materials Research and Testing
12200 Berlin, Germany

ABSTRACT

Finite element analysis (FEA) has been carried out for investigation of damping concrete under different impact loading conditions with a built-in material model and damage criteria available in FEA code ABAQUS.

At first, all parameters for the selected material model had been derived from compression tests of cubic specimens. After that, a validation was carried out with different static and dynamic penetration tests. Finally, a 5 meter real drop test with a 23 Mg cylindrical cask could successfully be simulated.

INTRODUCTION

A special concrete is used as energy absorbing foundation in interim storage facilities for casks loaded with radioactive material in Germany [1]. This so-called damping concrete is a concrete-polymer composite with a long plateau of nearly constant pressure vs. strain relations under pressure loading conditions. A series of impact and drop tests have been carried out at BAM to understand its mechanical behavior in accident scenarios. These tests included cubic specimen compression tests with or without clamping, penetration tests with different indenters, and a large scale test with a cylindrical object dropped onto a damping concrete foundation [2]. In parallel to the tests, numerical simulations based on the finite element method have been conducted. Results of these compression tests with cubic specimens under different load velocities, with or without clamping, have shown a very complex mechanical behavior. The most important characteristics are nonlinear elastic-plastic behavior with large volume change at the plateau zone at nearly constant pressure, pronounced hardening under clamping conditions after the plateau zone and very early damage under shear loading conditions without clamping. Additionally, all of these characteristics depend significantly on load velocity. Hence, numerical simulation of such material under different loading conditions is a challenging task. At first, a material model which provides the relevant features of damping concrete (like volume change, nonlinear elastic-plastic reaction, isotropic hardening, strain-rate dependency, ductile as well as shear damage including an evolution rule) must be found. Besides, this material model should be applicable under dynamic loading conditions. Numerical modeling aspects such as eroding contact and adaptive

meshing should also be considered with respect to material damage. A comparison of test results and simulation results proved that the built-in ABAQUS [3] crushable foam material model with isotropic hardening combined with shear and ductile damage can in principle be used to describe the complex mechanical behavior of the investigated damping concrete under the given impact loading conditions.

TEST RESULTS OF CUBIC SPECIMEN

The following results have been obtained from two different series of compression tests with cubic specimens with and without clamping. For the test series with clamping (confined compression tests) under different load velocities, the axial stress-axial strain relations are given in Figure 1a, while the lateral stress-axial strain relations are in Figure 1b [2]. Herby, the axial direction corresponds to the direction of displacement-controlled load input.

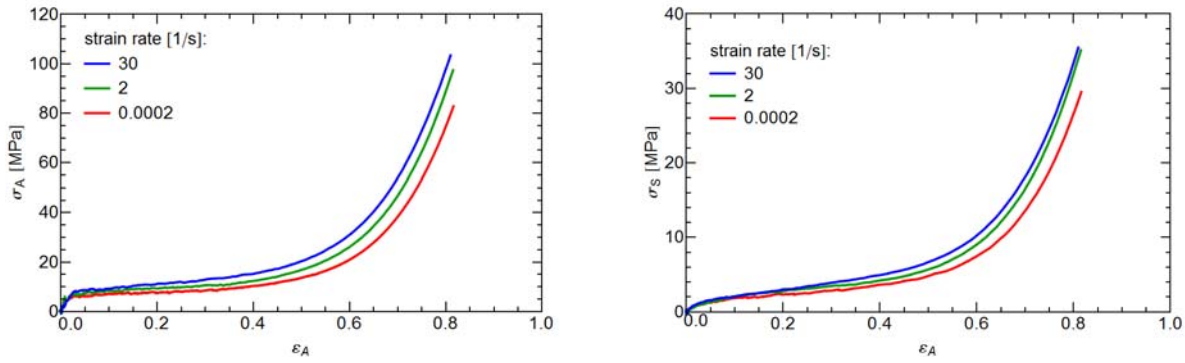

a) **b)**

Figure 1. Stress-strain curves for cubic specimens from confined compression tests with different load velocities

Hooke's law in axial (index "A") and lateral (index "S") direction is used for the calibration of the elastic modulus E and Poisson's ratio ν:

$$\varepsilon_A = \frac{1}{E}[\sigma_A - 2\nu\sigma_S], \tag{1}$$

$$\varepsilon_S = 0 = \frac{1}{E}[\sigma_S - \nu(\sigma_A + \sigma_S)] \tag{2}$$

With the measured σ_A, σ_S and ε_A from static confined compression test follows

$$\nu = \sigma_S / (\sigma_A + \sigma_S), \tag{3}$$

$$E = (\sigma_A - 2\nu\sigma_S) / \varepsilon_A \ . \tag{4}$$

Figure 2 presents the calculated curves according to equations (3) and (4). The elastic modulus and Poisson's ratio were determined graphically as ν=0.256 and E=560 N/mm² with the assumption that the material behaves linear elastic at beginning of the test.

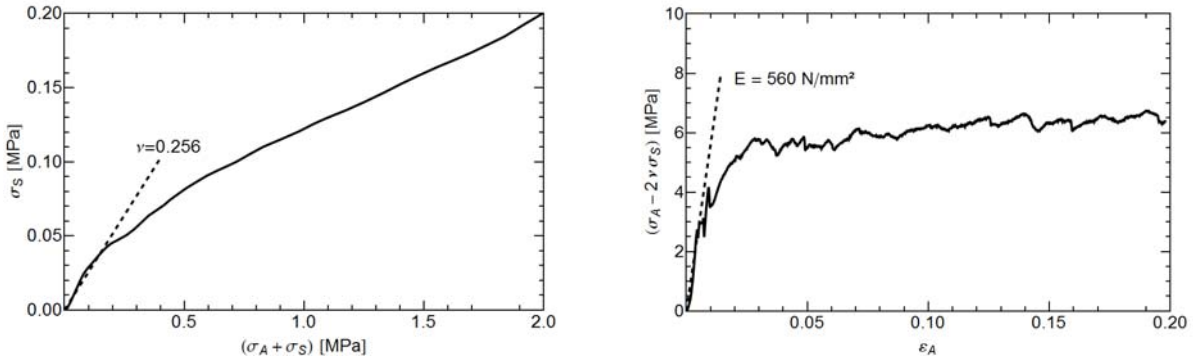

a) **b)**

Figure 2. Calculated curves according to equations (3) and (4)

Figure 3 shows the relation between effective (von Mises) stress

$$\sigma_q = \sigma_A - \sigma_S \tag{5}$$

and hydrostatic pressure

$$\sigma_m = (\sigma_A + 2\sigma_S)/3 \tag{6}$$

for the confined compression tests. In all of these tests its arithmetic average ratio σ_m/σ_q is $6/7$. This is important for parameter calibration of the material model as discussed below.

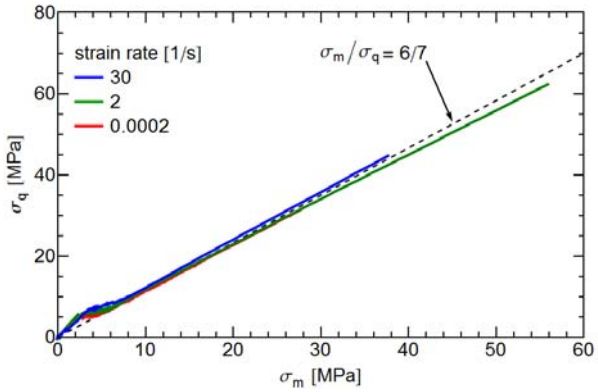

Figure 3. Relation between σ_q and σ_m for confined compression tests

Without clamping (uniaxial compression test), in contrast, the specimen yields a non-homogeneous stress and strain field. The mean stress-strain curves for these test series are shown in Figure 4. Material damage occurs very early at beginning of the test under significant shear load and very small pressure. The failure is accompanied by non-homogeneous micro cracking and localized plastic deformation of the specimen due to the random nature of the microstructure of damping concrete. Therefore, test results of uniaxial compression were used only for qualitative validation of the damage model.

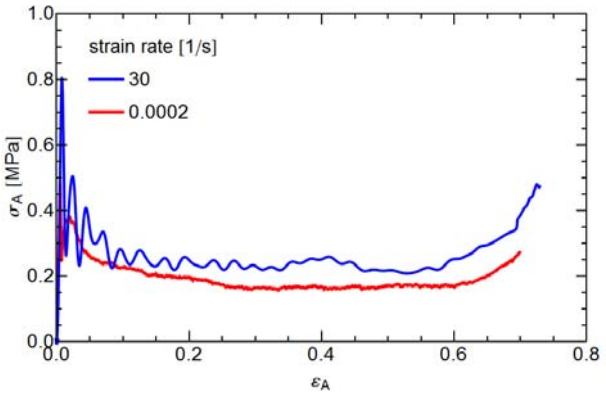

Figure 4. Mean stress-strain curves for cubic specimens from uniaxial compression tests with different load velocities

CALIBRATION OF MATERIAL PARAMETERS

Finite element code ABAQUS/Explicit [3] was used for the numerical simulations. It provides a crushable foam material model with isotropic hardening which had originally been developed for metal foams. Here it was applied to damping concrete assuming material homogeneity. The model separates the material behavior additively into a linear elastic part and a plastic part with hardening. The elastic part is defined by the parameters E = 560 N/mm² and ν = 0.256. For the plastic part, the yield surface has the form [3]

$$\sqrt{\sigma_q{}^2 + \alpha^2 \sigma_m{}^2} - \alpha \sigma_m^c = 0 \tag{7}$$

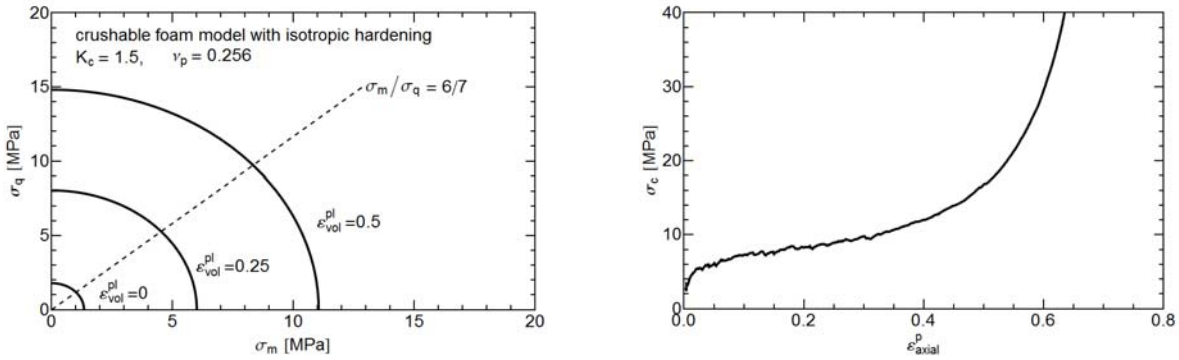

a) **b)**

Figure 5. Crushable foam plasticity model with isotropic hardening from ABAQUS for damping concrete in compression

where σ_m^c is the yield stress under hydrostatic pressure and

$$\alpha = \frac{3k_c}{\sqrt{9 - k_c^2}} \tag{8}$$

is a form-factor with

$$k_c = \sigma_c^0 / \sigma_m^{c0}. \tag{9}$$

Hereby, σ_c^0 is the initial yield stress from uniaxial compression and σ_m^{c0} is the initial yield stress from hydrostatic compression. The flow potential has the form

$$G = \sqrt{\sigma_q{}^2 + \beta^2 \sigma_m{}^2} \tag{10}$$

where β represents the shape of the flow potential ellipse on the meridional stress plane. It is a function of the plastic Poisson's ratio ν_p:

$$\beta = \sqrt{\frac{9(1-2\nu_p)}{2(1+\nu_p)}} \tag{11}$$

The yield surface and hardening curve for a constant ratio $\sigma_m / \sigma_q = 6/7$ (from confined compression tests) are given in Figure 5. For ratios $\sigma_m / \sigma_q < 6/7$ the material model predicts high flow stress under small pressure which is uncommon to damping concrete. Hence, the use of this material model for damping concrete requires additional damage criteria to change the shear and tension failure under small pressure and large shear.

DAMAGE CRITERIA

ABAQUS [3] provides various damage criteria. The main damage mechanisms needed here, have already been implemented: ductile damage due to nucleation and coalescence of polymer cells, and shear fracture due to shear band localization of the cement matrix. For ductile failure of damping concrete a simple Johnson-Cook [4] criterion

$$\varepsilon_D^{pl} = c_1 + c_2 e^{c_3 \eta}. \tag{12}$$

might be used with $c_1 = 10$, $c_2 = 10$, $c_3 = -2$ and $-1 < \eta < 1$, where ε_D^{pl} is the initial equivalent plastic strain and $\eta = -\sigma_m / \sigma_q$ is the stress triaxiality. Thus, critical plastic strain of initial damage decreases with increasing stress triaxiality. A more sophisticated model is the CrachFEM model [5] for thin sheets which extends material model no. 52 in FEA code PAMCRASH. For ductile failure the CrachFEM model assumes that the initial equivalent plastic strain at ductile failure depends only on the stress triaxiality as

$$\varepsilon_D^{pl} = d_0 e^{-3a_0\eta} + d_1 e^{3a_1\eta}. \tag{13}$$

Originally the criterion eq. (13) has only one constant parameter $a_0 = a_1 = a$. With $d_0 = 10$, $a_0 = 0$, $d_1 = c_2$ and $a_1 = c_3/3$ it is equal to the Johnson-Cook criterion eq. (12) what is shown in Figure 6a. For shear failure it is assumed in ABAQUS [3] that the equivalent plastic strain at the onset of damage is a function of the shear stress ratio. The shear stress ratio is defined as

$$\theta_s = \frac{\sigma_q}{\tau_{\max}}(1 - k_s \eta) \tag{14}$$

where $\tau_{\max}$ is the maximum shear stress (Tresca's stress) and k_s is a material parameter. If $k_s = 0$, the influence of compression in shear stress ratio is not considered. The CrachFEM assumes that the initial equivalent plastic strain at shear failure

$$\varepsilon_S^{pl} = d_2 e^{-f_2\theta_s} + d_3 e^{f_3\theta_s} \tag{15}$$

depends on shear stress ratio as it depends on stress triaxiality at ductile failure. Again, the original criterion has only one constant parameter $f_2 = f_3 = f$. Figure 6b shows the criterion for $k_s = 0$, $d_2 = -4.33$, $d_3 = 8.744 \cdot 10^{-9}$, $f_2 = 0$ and $f_3 = 11.567$ for $\sqrt{3} \le \theta_s \le 2$.

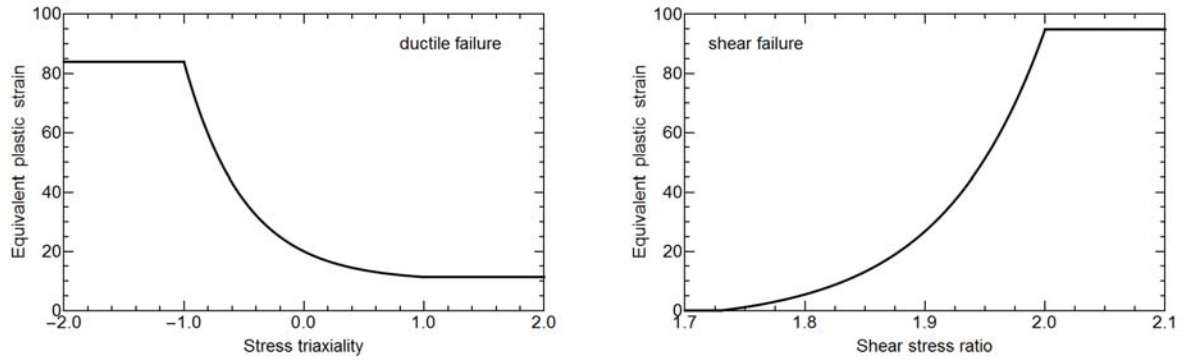

a) **b)**

Figure 6. Ductile (a) and shear (b) damage initiation criteria for damping concrete

SIMULATION OF COMPRESSION TEST

The simulation results of the confined compression test with and without application of damage criteria are compared with test results in Figure 7. Calculated axial forces are quite similar to measured forces when the hardening curve of the material model is adjusted to the experimental results. Lateral forces show some differences. Altogether, the crushable foam model gives acceptable results for forces in axial as well as lateral direction. The damage criteria have, necessarily, no influence on the simulation results for confined compression test.

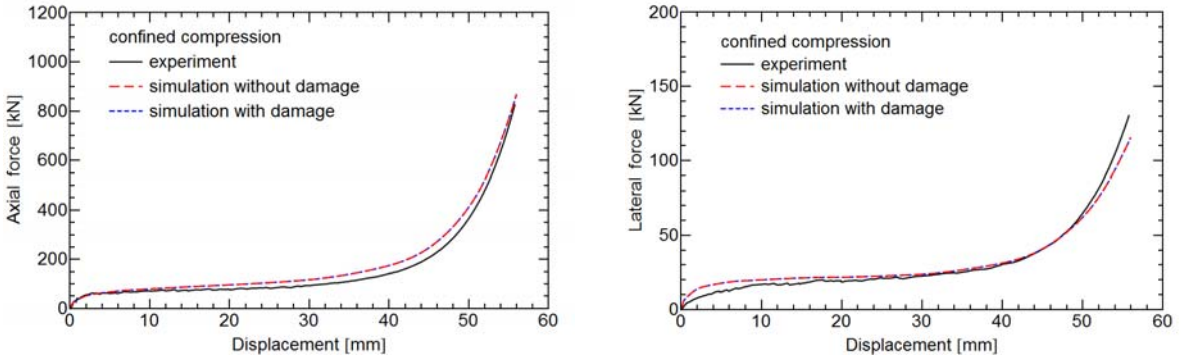

a) **b)**

Figure 7. Comparison of test results with computational results of static compression test with and without damage criteria

SIMULATION OF PENETRATION TEST

One static penetration test and six dynamic penetration tests were conducted at a hydraulic compression testing machine respectively at the test machine for guided drop tests to verify the material model for a drop test scenario and to learn more about the failure process of damping concrete.

The static test was carried out with a 200x200x200mm³ cubic specimen clamped in a steel box. The indenter had a 100x100mm² cross-section area. It penetrated into the specimen with constant velocity of approx. 0.5 mm/s causing a significantly increasing reaction force up to locking.

Calculation results show a good agreement of global deformation with test results (Figure 8a) up to locking. After that, the curves differ more and more (Figure 8b) because of deficiencies in damage modeling. Obviously, more experimental data of triaxial tests are needed to improve the damage criteria. In this simulation the eroding contact feature was used, i.e. at ductile/shear failure new contact surfaces between failed elements as well as between penetrated elements and indenter were automatically generated.

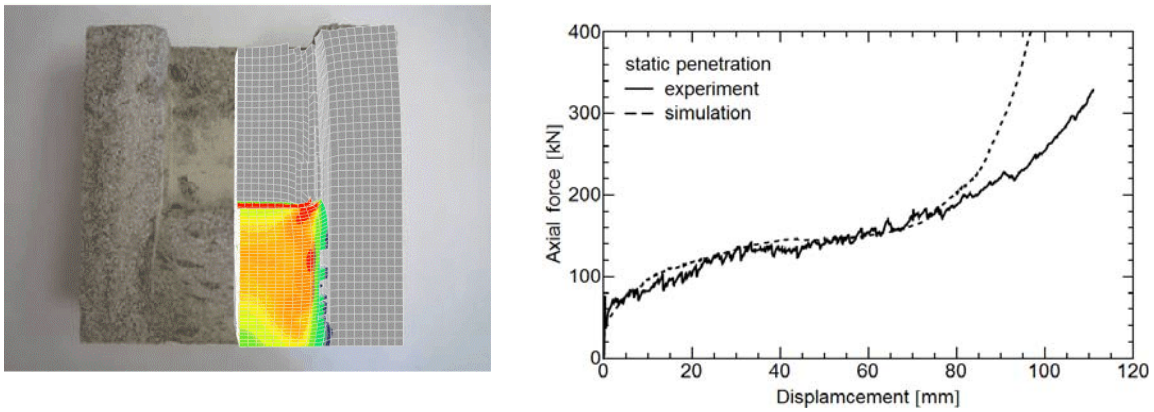

a) **b)**

Figure 8. Static penetration test with cubic specimen

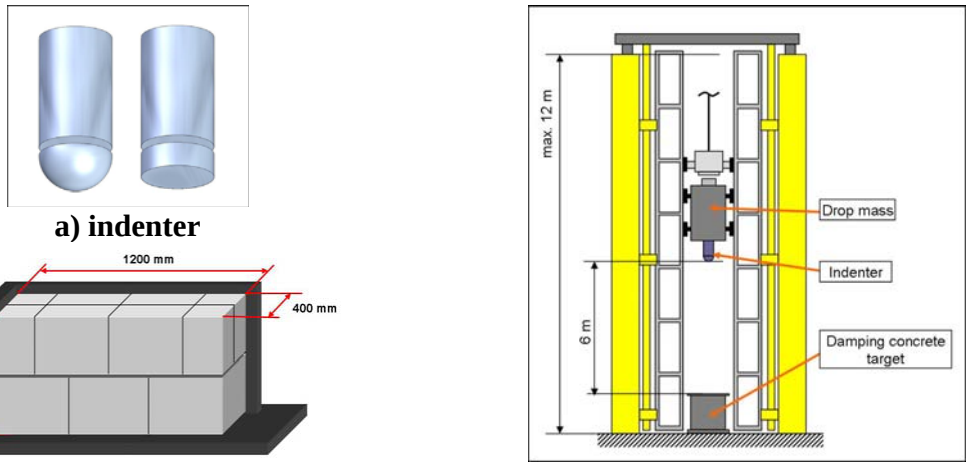

a) indenter

b) target box **c) guided drop test stand**

Figure 9. Equipment of penetration test

The dynamic tests [2] shown in Figure 9 were conducted with two different indenters: a cylindrical body with plane front, and a cylindrical body with hemispherical front. Each indenter was put below the drop weight with total mass of 1100 kg. The drop height was 6 meter. Two targets were built up with damping concrete bricks of defined orientation in 1200x400x500mm³ steel boxes. The boxes had a wall thickness of 10 mm and were fixed on top of the test stand foundation of the BAM guided drop test facility. Each target was used for three drop tests using different positions of the box surface. Altogether six tests were conducted, two of them with plane front and four with hemispherical front. Further tests with the same as well as varying configurations are currently under preparation in order to improve the reliability of the results and to study relevant factors such as drop height and friction.

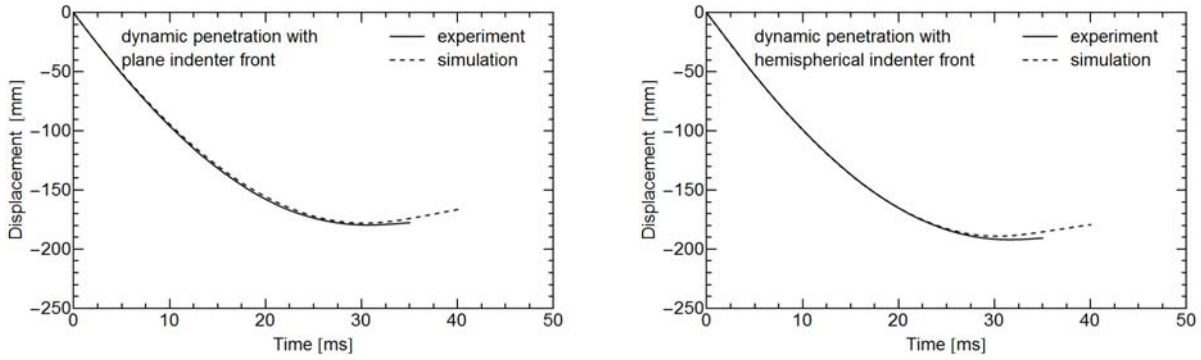

a) **b)**

Figure 10. Measured and calculated penetration depths from indenter with plane front (a) and indenter with hemispherical front (b)

Figure 10 illustrates the test results and corresponding calculation results. The curves show penetration depth over time for a 6 m drop with plane indenter (Figure 10a) and hemispherical indenter (Figure 10b). In both tests a penetration depth of about 175 mm and penetration time of about 30 ms is obtained. Even though the indenter geometry differ, the main damage mechanism turn out to be the same. Failure takes place only around the indenter tip during the penetration process. Damping concrete beneath the indenter is highly compressed, but material outside the failure zone shows almost no deformation. The calculated value of penetration depth meets the measured value for the plane indenter and is a little bit higher for the hemispherical indenter. After the maximum penetration, calculation shows an earlier rebound of the indenter than the test because of the complex friction process between damping concrete and steel indenter that has not yet been modeled. Pressure and temperature dependent slip/stick friction should be considered in the future.

DEMONSTRATION TEST

A 5 meter drop test with a 23 Mg cylindrical cask was conducted to verify the developed material model under real drop test conditions. The drop test target is a 2400x2400x500mm³ block of damping concrete confined in a rigid steel frame. A 30 mm thick mortar layer was applied between damping concrete and the steel slab of the IAEA target at the BAM drop test facility (Figure 11a).

a) **b)**

Figure 11. Drop test scenario with a cylindrical cask on top of the 500 mm thick damping concrete block

A description of this drop test is presented in Ref. [2]. The detailed finite element model of the whole drop test scenario including cask (as rigid body with a concentrated mass), damping concrete block, steel frame, mortar layer and IAEA target is shown in Figure 11b. The model of the IAEA target was already used for simulations of various other drop tests scenarios [6], [7], [8] and [9]. Using the above given material parameters the simulation was carried out with an initial velocity of 9.9 m/s of the cask body onto the damping concrete block. The comparison of Figure 12a and 12b shows a good correspondence between drop test and simulation results.

a) **b)**

Figure 12. Imprint of the cylindrical cask into the damping concrete block after 5 meter drop test.

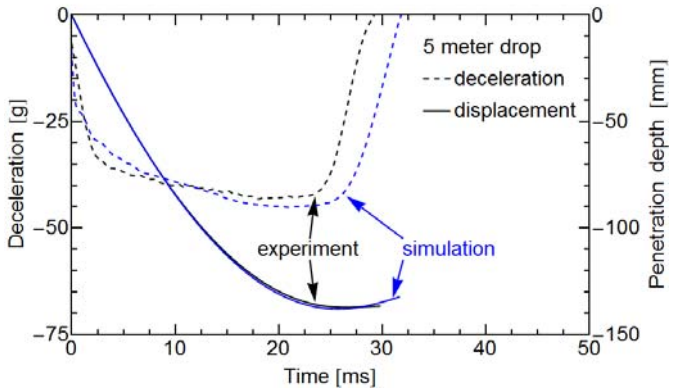

Figure 13. Calculated and measured deceleration and penetration depth at 5 m drop test

As presented in Figure 13, the calculated maximum rigid body deceleration of about 46 g (1g = 9.81 m/s²) is somewhat higher than the measured cask body deceleration of 43 g. Maximum penetration depth of about 134 mm corresponds to the measured value of about 132 mm quite good. However, the rebound of the cask body found in the simulation did not occur in reality.

CONCLUSIONS

A FEA code ABAQUS built-in material model for isotropic crushable foam combined with additional damage criteria for ductile as well as shear failure was used to describe the mechanical behavior of damping concrete under impact loading conditions. Microscopic effects of this material such as softening or hardening associated with the collapse of individual polymer cells or separation of polymer cells from the mortar matrix cannot be considered with this macroscopic material model from continuum mechanics. But the main features such as volume

change, hardening under compression and low shear strength of this material which dominate the global behavior under impact conditions are contained in the model.
Some effects of damping concrete are still unknown; others cannot be described with ABAQUS built-in material models. For example, modeling of strong hardening between 50 % and 80 % volume change in combination with very low tension or shear failure stress (< 1MPa) should be improved. Therefore, further tests are necessary to learn more about this complex material, especially the failure process.
This work provides a phenomenological basis for the development of a new user-defined material model of damping concrete which could be used in future for safety assessments of different casks subjected to severe impact scenarios in nuclear facilities of Germany.

ACKNOWLEDGEMENTS

The authors wish to acknowledge the financial support of the research project ENREA from the German Federal Ministry of Education and Research under contract no. 02S8588.

REFERENCES

1. Kasparek, E. et al.: Studies in search of the most appropriate impact limiter material, 17th Int. Symposium on the Packaging and Transportation of Radioactive Materials (PATRAM 2013), San Francisco, CA, USA, August 18-23, 2013.
2. Scheidemann, R. et al.: Model-sized and full-scale dynamic penetration tests on damping concrete, 17th Int. Symposium on the Packaging and Transportation of Radioactive Materials (PATRAM 2013), San Francisco, CA, USA, August 18-23, 2013.
3. ABAQUS Analysis User´s Manual, Version 6.12, Dassault Systémes, 2012.
4. Johnson, G. R., Cook, W. H.: Fracture characteristics of three metals subjected to various strains, strain rates, temperatures and pressures. Engineering Fracture Mechanics, Vol. 21, No. 1, pp 31-48, 1985.
5. Gese, H. et al.: CrachFEM – a comprehensive failure model for metallic structures in sheet metal forming and crash simulation, Proc. EuroPAM, Paris, France, Oct. 11-13, 2004.
6. Qiao, L., Zencker, U., Wieser, G., Völzke, H.: Numerical safety assessment of a transport and storage cask for radioactive materials without impact limiters by the 0,3m drop test onto an unyielding target, Proc. 9th International Conference on Computational Structures Technology, Athens, Greece, September 2-5, 2008.
7. Qiao, L., Zencker, U., Wille, F., Musolff, A.: Numerical simulation of 9 meter drop of a transport and storage cask with aluminium impact limiter, Proc. 16th Int. Symposium on the Packaging and Transportation of Radioactive Materials (PATRAM 2010), London, UK, October 3-8, 2010.
8. Qiao, L., Zencker, U., Musolff, A., Komann, S.: Dynamic finite element analyses of a spent fuel transport and storage cask with impact limiters by 9 meter drop tests, Proc. SIMULIA Customer Conference 2011, Barcelona, Spain, May 17-29, 2011.
9. Qiao, L., Zencker, U. et al.: Numerical investigation of a complex drop test scenario, Radioactive Materials Transport and Storage Conference and Exhibition (RAMTRANSPORT 2012), London, UK, May 23-24, 2012.